Heliyon 9 (2023) e17242

Contents lists available at ScienceDirect

Heliyon

journal homepage: www.cell.com/heliyon

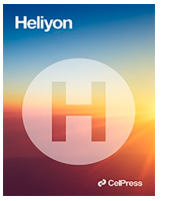

Spatial distribution of selenium and other potentially toxic elements surrounding mountaintop coal mines in the Elk Valley, British Columbia, Canada

Wyatt Petryshen

Wildsight, Kimberley, British Columbia, Canada

ARTICLE INFO

Keywords:
Mosses
Fugitive dust
Air quality
Deposition
Community health
Biomonitoring

ABSTRACT

Despite the extensive use of mountaintop coal mining in the Elk Valley, British Columbia, Canada's largest metallurgical coal-producing region, little is known about the transport and deposition of fugitive dust emissions within its mountain landscape. This study aimed to assess the extent and spatial distribution of selenium and other potentially toxic elements (PTEs) near the town of Sparwood originating from fugitive dust emitted from two mountaintop coal mines. To achieve these objectives concentrations of 47 elements within moss tissues of *Hylocomium splendens*, *Pleurozium schreberi*, and *Ptilium crista-castrensis* were analyzed from 19 locations between May 29 to June 1, 2022. Contamination factors were then calculated to identify areas of contamination, along with generalized additive models to assess the relationship between selenium and the mines. Finally, Pearson correlation coefficients were calculated between selenium and other PTEs to determine which exhibited similar behaviour. This study found that selenium concentrations are a function of proximity to mountaintop mines, and the region's topographic features and prevailing wind patterns play a role in the transport and deposition of fugitive dust. Contamination is highest immediately surrounding mines and decreases at increasing distances, with the region's steep mountain ridges shielding the deposition of some fugitive dust when acting as a geographic barrier between adjacent valleys. Furthermore, silver, germanium, nickel, uranium, vanadium, and zirconium were identified as other PTEs of concern. The implications of this study are significant as it demonstrated the extent and spatial distribution of contaminants originating from fugitive dust emissions surrounding mountaintop mines and some of the controls to its distribution in mountain regions. As Canada and other mining jurisdictions look to expand critical mineral development, it will be important for proper risk assessment and mitigation in mountain regions to limit community and environmental exposure to contaminants within fugitive dust.

1. Introduction

Mountaintop removal (MTR) coal mining has been associated with serious environmental and community health impacts [1,2]. Epidemiological studies have reported that persons living near MTR coal mines experience significantly higher rates of morbidity and mortality from cardiovascular disease, kidney disease, respiratory disease, dental disease, and cancer compared to persons not living near coal mining operations [2]. Factors leading to these poor health outcomes originate from reductions in air, soil, and water quality,

E-mail address: wyatt@wildsight.ca.

https://doi.org/10.1016/j.heliyon.2023.e17242
Received 5 June 2023; Received in revised form 9 June 2023; Accepted 12 June 2023
Available online 27 June 2023

increases in fine air particulate and ambient silica, and exposure to polycyclic aromatic hydrocarbons and cleaning chemicals [2]. Reductions in air quality can occur during mining operations such as blasting, coal processing, dumping of coarse refuse, rail loading, and wind erosion of storage piles, resulting in the aerial transport and deposition of potentially toxic elements (PTEs), which can negatively impact flora, fauna, and human health [3,4]. Elements of concern include heavy metals like silver (Ag), cadmium (Cd), nickel (Ni), lead (Pb), selenium (Se), uranium (U), and vanadium (V) [5,6].

In the Elk Valley of British Columbia (B.C.), Canada, mountaintop coal mines have been found to impact downstream environments, crossing international boundaries. Research has found that these mines are a primary source of Se and other contaminants into the Elk River and its tributaries, increasing the loadings of Se to these waterbodies through time [7,8]. Recent work by Cooke and Drevnick (2022) extended the impacts from these mines to include adjacent downwind watersheds through the analysis of a sediment core collected from Window Mountain Lake, Alberta, approximately 12 km east of the Elkview Mine, across the Continental Divide [9]. Analysis of this sediment core revealed increased concentrations of polycyclic aromatic compounds (PACs) and Se that corresponded to increased coal mine production. Cooke and Drevnick (2022) identified the source of contamination being fugitive dust emitted during mining operations and transported by winds [9]. Air-quality monitoring stations are deployed in the Elk Valley at five locations monitoring particulate matter (PM_{10}, $PM_{2.5}$), nitrogen dioxide (NO_2), and ozone (O_3), however, there is no environmental monitoring of heavy metals that may be aerially deposited in fugitive dust emissions. A gap exists in our knowledge of contamination from fugitive dust emissions within this region and how it may impact community and environmental health. Refining our understanding of how fugitive dust is transported and deposited from mountaintop mines in mountainous regions is critical for policymakers and the general public, especially as Canada and other mining jurisdictions look to expand critical mineral development.

The objectives of this study were to evaluate the extent and spatial distribution of Se and other PTEs originating from fugitive dust emitted from the Elkview and Line Creek mines, in the Elk Valley, B.C., using moss biomonitoring. Moss biomonitoring is a widely used

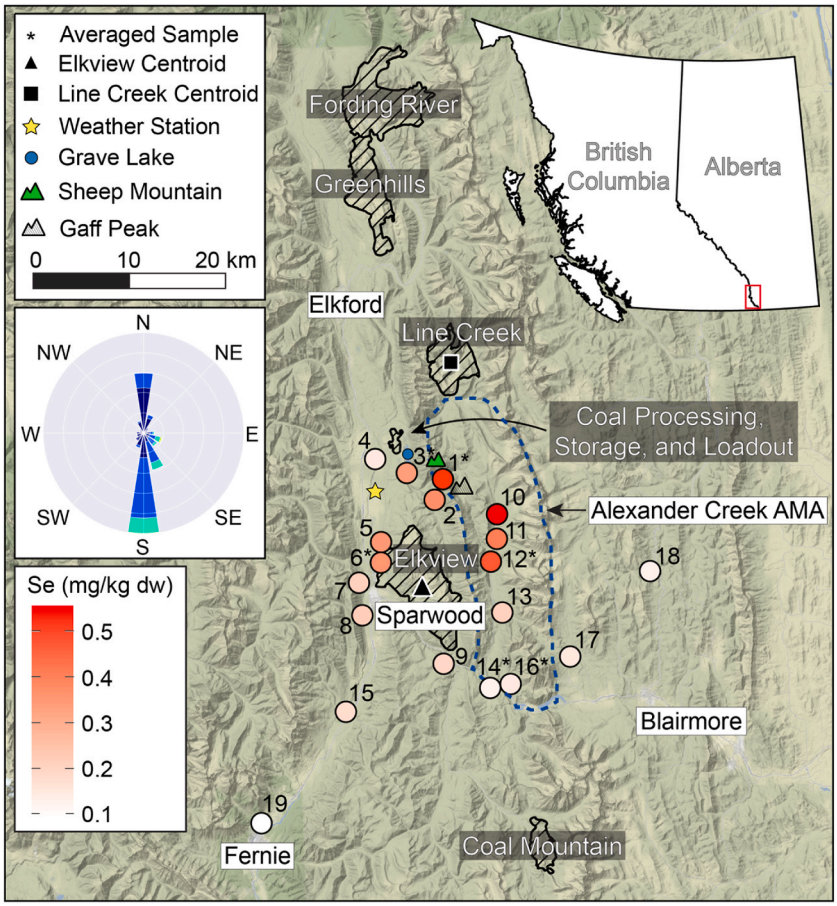

Fig. 1. (*in color*). Map of the study area with selenium concentrations at sample locations. Operating mountaintop coal mines include the Fording River, Greenhills, Line Creek, and Elkview mines. Coal processing, storage, and loadout for the Line Creek Mine is indicated on the map along with the approximate boundaries for the Alexander Creek Access Management Area (AMA). The Coal Mountain Mine is in closing and reclamation. Sampling was completed around the town of Sparwood and the Elkview Mine. Sites 17 and 18 are in Alberta, while the remainder are in British Columbia. Sites with asterixis represent averaged samples. Wind rose data (January 2020–May 2022) was retrieved from the Government of Canada at the Sparwood Airport (yellow star; https://climate.weather.gc.ca/index_e.html). (For interpretation of the references to color in this figure legend, the reader is referred to the Web version of this article.)

technique that has been successful in assessing the temporal and spatial distribution of atmospheric pollution, with studies in Europe since the 1970's, in Asia, Africa, North America, and in Canada [10–23]. Moss biomonitoring offers a cost-effective and easy-to-implement methodology due to the ability to assess multiple elements at a single location and to constrain timeframes of deposition to the last 2–3 years [20,24]. The concentrations of PTEs are retrieved through the analysis of living portions of moss since certain species of moss uptake nutrients directly from the atmosphere, incorporating atmospheric pollution directly into their tissues [17]. The objectives of this study were achieved by: (1) analysis of moss tissue from 19 locations in the study area to determine elemental concentrations; (2) the calculation of contamination factors to understand the extent of contamination as compared to the reference location; (3) the determination of the relationship between the distance and azimuth of the Elkview and Line Creek mines to Se contamination factors within the study area using generalized additive models (GAMs); and (4) the calculation of Pearson correlation coefficients between Se and other PTEs to identify which elements exhibited similar behaviour.

2. Materials and methods

2.1. Study area

The Elk Valley of southeastern B.C., Canada, covers an area of approximately 3568 km^2 [25]. The valley is approximately 150 km in length and typically varies in width between 1 and 5 km, bordered by the Rocky Mountains to the east and west. The valley has been home to coal mining for over 100 years, with four currently operating mountaintop mines, one mine in closing and reclamation, and four proposed. Coal deposits within the Elk Valley consist of high-to low-volatile bituminous coal from the Mist Mountain Formation of the Jurassic-Cretaceous Kootenay Group [26]. The Elk Valley's current operating mines produce between 20 and 25 million tonnes of coal per year, accounting for 80% of Canada's total annual metallurgical coal exports [27]. Waste rock produced during the mining process includes interbedded siltstones, mudstones, and unminable coal seams within the Mist Mountain Formation, along with underlying rocks from the Morrissey and Fernie formations, and the overlying Elk Formation [28]. As of 2022, the cumulative volume of waste rock stored in dumps is 6739 million bank cubic meters [29]. The mean Se concentrations within all waste rock are 3.12 ± 1.43 mg/kg with no significant difference between samples from individual dumps or between dumps of the Mist Mountain Formation with exception of samples from the Fording River Operations [28]. Selenium bearing minerals found in pre- and fresh-blast samples include pyrite, sphalerite, chalcopyrite, and barite, with Fe oxyhydroxides occurring as a secondary mineral in waste rock dumps [28]. Trace elements such as As, Cd, Cr, Ni, and Zn are often associated with primary sulfide minerals within coal waste rock dumps [30]. The geochemistry of coals within the Mist Mountain Formation are also relatively consistent, with variations in element concentrations linked to changes in ash content, geological setting, degree of weathering, and depositional environment [31].

Major population centers in the valley include the towns of Elkford (district population: 2749), located approximately 5 km southwest of the Greenhills Mine and 10 km northwest of the Line Creek Mine, Sparwood (district population 2021: 4148), located under 3 km from the Elkview Mine, and Fernie (district population 2021: 6320), located approximately 30 km southwest of the Elkview Mine (Fig. 1) [32]. The prevailing wind patterns at the Sparwood airport are north-south with a portion trending southeast. The Elk Valley contains 13 biogeoclimatic subzone variants of Engelmann Spruce – Subalpine Fir, Montane Spruce, Interior Cedar Hemlock, Ponderosa Pine, Interior Douglas Fir, and Interior Mountain Alpine [25].

The largest point-source emitters of fugitive dust emissions in the valley are the region's mountaintop coal mines, which Cooke and Drevnick (2022) reported as the main source of PACs and Se (Fig. 1) [9,33]. Other potential sources of fugitive dust originate from industrial forestry, major highways, dirt roads, and rail transport lines.

2.2. Sample collection

Between May 29 to June 1, 2022, 19 locations were sampled for *Hylocomium splendens*, *Pleurozium schreberi*, and *Ptilium crista-castrensis*. Twenty-three locations were initially sampled with 4 excluded due to insufficient sample weight or outlier elemental concentrations (Figures SI4, SI5, Table SI2). These species were chosen as biomonitors due to their relative abundance, easy identification, and widespread use in other biomonitoring studies [15,17,24]. Moss colonies were typically found growing on the ground, on deadfall, on tree stumps, or in tall, sparse grasses.

The study area was initially confined to a 625 km^2 grid centered over the Elkview Mine (approx. 3.2 km $\times$ 3.2 km grid boxes; Figure SI1). Attempts were made to sample as many of the grid boxes as possible with the main limiting factors being access, early spring snow conditions, proximity to paved roadways, moss availability, and topography (Figure SI1). Large portions of the grid also included privately owned land and ecosystems not favorable to our target moss species, further making sample collection difficult. Sampling in this study was thus not random and unaccounted biases may have impacted site selection. The sample distribution also precluded the examination of fugitive dust emitted from the Fording River Mine and Greenhills Mine, which likely contribute a significant amount of fugitive dust to the region. Of the 64 grid boxes, 14 were successfully sampled, with 1 yielding no results after analysis. Four sample locations were also located outside of the grid (Figure SI1). Fernie was chosen as the reference location since it is located approximately 30 km southwest of the Elkview Mine, outside the typical area that would expect impacts from fugitive dust emissions.

Specific sample locations were chosen by driving into accessible grid boxes and hiking until the target species was identified. Following ICP Vegetation (2015) sampling protocols, attempts were made for samples to be located at least 300 m away from paved roadways and at least 100 m away from moderately trafficked dirt roads [24]. Sample 6 was near a rail transport line. Most samples were collected from sites that were either open or had low canopy cover. At each sample location, at least 5 sub-samples were collected

from an approximately 50 m × 50 m area and combined to create a representative sample. Moss samples were picked using disposable powder-free polyethylene gloves to avoid contamination and placed into 1 L plastic Ziplock bags. Only living portions of moss were picked, with ground litter and dirt removed. Samples were then sorted a second time to remove any dead portions of moss, dirt, or ground litter, before being sent for analysis.

Duplicate and triplicate samples were also collected consisting of either *H. splendens* or *P. schreberi,* or if *P. crista-castrensis* was sampled, *P. crista-castrensis* and either *H. splendens*, *P. schreberi*, or both. These duplicate and triplicate samples were collected for locations 1 and 6, consisting of triplicate samples of *H. splendens*; location 3 of *H. splendens*, *P. schreberi*, and *P. crista-castrensis*; locations 12 and 16 of *P. schreberi* and *P. crista-castrensis*; and location 14 of *H. splendens, P. schreberi*, *H. splendens* (Table SI1). Mean (averaged) PTE concentrations from duplicate and triplicate samples were used within the analysis for each of the above locations. The primary motivation for collecting duplicate and triplicate samples at some of the locations was to assess the relative variation in PTE concentrations between different moss species and for individual samples at a given location, especially since this study utilized multiple moss species (Figure SI2).

Unfortunately, moss standard reference samples as recommended by ICP Vegetation (2015) were not obtained and sent for analysis due to time and financial constraints [24]. Aboal et al. (2017) and Świsłowski et al. (2021) provide an assessment of how different collection and processing techniques impact the overall measurement uncertainty and concentrations of heavy metals in moss biomonitoring studies [34,35].

2.3. Multi-element analysis

Multi-element analysis of moss samples was completed at ALS Global Vancouver, using inductively coupled plasma – mass spectrometry (ICP-MS) and inductively coupled plasma – atomic emission spectroscopy (ICP-AES). Prior to analysis, samples were dried for 24 h at 40 °C and fully milled below 1 mm, producing a homogenous sample. Prepared samples were then cold digested in nitric acid for 8 h, then heated in a graphite block for 3 h, before being brought to analysis volume with hydrochloric acid. Samples were then mixed thoroughly and analyzed using both ICP-MS and ICP-AES before being corrected for inter-element spectral interferences. The full analytical methodology and results are included in the GitHub repository.

2.4. Data analysis

The concentration data of the 47 elements from the moss samples were analyzed in R Studio running R version 4.1.2 (2021) [36, 37]. QGIS version 3.22 was used to calculate the centroid location for the Elkview and Line Creek mines, and the distances from the mine centroids to the sample locations [38]. Python version 3.9.7 was used to calculate the azimuth direction from the Elkview and Line Creek mine centroids to each sample location, and to produce the wind rose diagram in Fig. 1.

Summary statistics for each element (mean, median, minimum, maximum, variance, standard deviation, coefficient of variation, skewness, and kurtosis) were calculated and can be found in the supplementary information data file. Samples 1, 6, and 18 had insufficient sample weights and were excluded from further analysis. Concentrations of ln, Na, Pd, Pt, Re, and Te were also predominantly below sample detection limits and excluded from further analysis (53 initial elements analyzed with 47 having complete results). Only elements that were above sample detection limits for all locations were included. A boxplot of Se concentrations grouped by moss species is presented in Figure SI3.

Contamination factors (CFs) for each analyzed element were then calculated for all locations using Fernie, location 19, as the background reference location. Contamination factors are useful as they can be used to identify if concentrations of an element are indicative of contamination as compared to normal ambient conditions, independent of if they cause environmental harm [39,40]. Contamination factors are calculated as the ratio between the element concentration in a sample divided by the background concentration at the reference location [41]. Contamination factors are then subdivided into six categories according to the CF value: no contamination (CF1; CF less than 1), suspected contamination (CF2, CF between 1 and 2), slight contamination (CF3, CF between 2 and 3.5), moderate contamination (CF4, CF between 3.5 and 8), severe contamination (CF5, CF between 8 and 27), and extreme contamination (CF6, CF greater than 27) [41]. Boxplots of CFs for each of the elements were used to identify potential outlier samples (Figures SI4, SI5). Mean PTE concentrations were then calculated for any locations with duplicate or triplicate samples and used in further analysis (see supplementary information data file).

To determine the relationship between Se CFs at locations throughout the study area and the Elkview and Line Creek mines, generalized additive models (GAMs) using the R package "mgcv" was used [42]. GAMs are a flexible model type that can fit complex non-linear relationships between the response variable and the explanatory variables. In this study, the response variable, Se CFs, was modelled to two explanatory variables, distance and azimuth from either the Elkview Mine or Line Creek Mine. Additionally, two linear regressions were completed for samples within the Alexander Creek Access Management Area (AMA) between Se CFs and the distance from the Line Creek Mine and Elkview Mine (Figures SI6, SI7; supplementary information). Interaction effects between the distance and azimuth covariates were not examined due to the limited number of observations. A Tweedie distribution with an identity link function was chosen for each of the models, with a thin plate spline function used to fit the distance variables and a cyclic cubic regression spline function to fit the azimuth variable for the Elkview Mine GAM. For the azimuth variable in the Line Creek Mine GAM, a thin plate spline function was used instead of a cyclic cubic regression spline function since samples were only collected from azimuth directions between 140° and 220°. The smoothing parameters were selected using the Restricted Maximum Likelihood standard (REML) method. The formula for the Elkview Mine GAM (Equation (1)) and the Line Creek Mine GAM (Equation (2)) were written as follows:

$$\mathrm{Se} \sim \mathrm{s(Distance)} + \mathrm{s(Azimuth, bs = 'cc')}, \mathrm{method} = \text{'REML'}, \mathrm{family} = \mathrm{tw(link = 'identity')} \quad (1)$$

$$\mathrm{Se} \sim \mathrm{s(Distance)} + \mathrm{s(Azimuth)}, \mathrm{method} = \text{'REML'}, \mathrm{family} = \mathrm{tw(link = 'identity')} \quad (2)$$

An alpha value of 0.05 was used to assess the significance of the variables in each of the GAMs along with deviance explained to assess the overall performance of the model.

Finally, to identify other PTEs that exhibited similar behavior to Se, Pearson correlation coefficients were calculated. Elements that were highly correlated and significant ($\alpha < 0.05$) would likely have similar origins to Se. Factor analysis could not be completed within this study due to the low number of observations ($n = 19$) compared to the 47 elements analyzed but could provide an avenue for future work if sample numbers are increased.

3. Results and discussion

3.1. Elemental concentrations and contamination factors

In total, the concentrations of 47 elements in samples of *H. splendens*, *P. schreberi,* and *P. crista-castrensis* were analyzed. Summary statistics for Ag, Cd, Cs, Ni, Pb, Sb, Se, and V are shown in Table 1 with a full table provided in the supplementary information data file. The top 5 elements with the highest mean concentrations were: Fe (785 mg/kg dw) > Mn (105 mg/kg dw) > Ba (67 mg/kg dw) > Zn (30 mg/kg dw) > Sr (13 mg/kg dw). All elements had coefficients of variation (CV) greater than 20%, indicating moderate (21% < CV ≤ 50%) to high variability (CV > 51%) with sample 11 being the only sample with anomalously high concentrations of As, Co, Li, and Fe, comprising 45% of all outlier points (Figures SI2, SI3). As such, sample 11 was excluded from further analysis (Table SI2). Selenium concentrations ranged from 0.09 mg/kg dw to 0.56 mg/kg dw with a mean value of 0.26 mg/kg dw and median of 0.21 mg/kg dw (Table 1). The reference sample collected from Fernie had a Se concentration of 0.09 mg/kg dw (Fig. 1).

The top three contaminants within this study and their respective maximum contamination factors (CFs) were Se (CF = 5.90), Ag (CF = 4.25), and U (CF = 4.06). Of the 47 elements analyzed, 20 elements from sample locations within this study fell into the moderate (CF4) to slight (CF3) contamination level as compared to the reference sample collected in Fernie (supplementary information data file). The highest concentrations of contaminants occurred predominantly within the narrow valley south of the Line Creek Mine in the Alexander Creek AMA (samples: 10, 11, 12; Fig. 1). Samples that were located between the two mines, near Grave Lake, or within the pass between Sheep Mountain and Gaff Peak also had high concentrations of contaminants (samples: 1, 2, 3; Fig. 1). Samples adjacent and directly east of the Elkview Mine, surrounding Sparwood, also contained elevated concentrations of Se and other PTEs (samples: 5, 6, 7, 8; Fig. 1).

3.2. Association between selenium contamination and mountaintop coal mines

For each of the constructed generalized additive models (GAMs), both the distance and azimuth covariates from the Elkview and Line Creek mines were significant in explaining Se CFs throughout the study area (Fig. 2). For the Elkview GAM, the distance covariate had a significant (p-value = 0.01) and weakly non-linear (Edf = 1.24) relationship to Se contamination, whereby Se contamination decreased as distance increased from the mine (Fig. 2a). For the azimuth covariate, it was also significant (p-value « 0.01) and non-linear (Edf = 3.22), with the maximum Se contamination occurring between approximately 315°–100° or in the northeast direction from the mine. The main peak at approximately 35° was asymmetrical, with a steep decline in Se contamination preceding 100°, but with a more gradual increase in Se contamination approaching 315° (Fig. 2b). For the Line Creek GAM, the distance covariate had a significant (p-value « 0.01) and non-linear (Edf = 3.86) relationship to Se contamination, similar to the distance covariate for the Elkview GAM, whereby Se contamination decreased as distance from the Line Creek Mine increased (Fig. 2c). However, the distance covariate in the Line Creek GAM was more non-linear when compared to the distance covariate in the Elkview GAM, which likely corresponds to a flat portion in the curve up to approximately 20,000 m from the mine whereby the slope of the curve is approximately zero (Fig. 2c). The increased non-linearity for the distance covariate in the Line Creek GAM was likely due to the lack of samples taken

Table 1
Summary statistics for Ag, Cd, Ni, Pb, Se, U, and V (mg/kg dw) from samples of moss tissue within the study area. A full table of the summary statistics can be found in the supplementary information data file. This table excludes sample 11.

Summary Statistics	Ag	Cd	Ni	Pb	Se	U	V
Number of samples	19	19	19	19	19	19	19
Minimum	0.02	0.10	1.43	0.63	0.09	0.03	1.03
Maximum	0.09	0.45	5.31	2.14	0.56	0.13	5.74
Reference site	0.02	0.32	1.52	1.00	0.09	0.03	1.66
Variance	0.00	0.01	1.22	0.16	0.02	0.00	1.82
Median	0.04	0.21	2.09	1.32	0.20	0.06	2.58
Mean	0.04	0.22	2.50	1.29	0.26	0.07	2.91
Standard deviation	0.02	0.09	1.10	0.40	0.14	0.03	1.35
Coefficient of variation (CV)	0.46	0.39	0.44	0.31	0.52	0.48	0.46
Skewness	0.63	0.74	1.09	0.34	0.66	0.45	0.74
Kurtosis	2.67	3.74	3.28	2.40	2.27	1.97	2.70

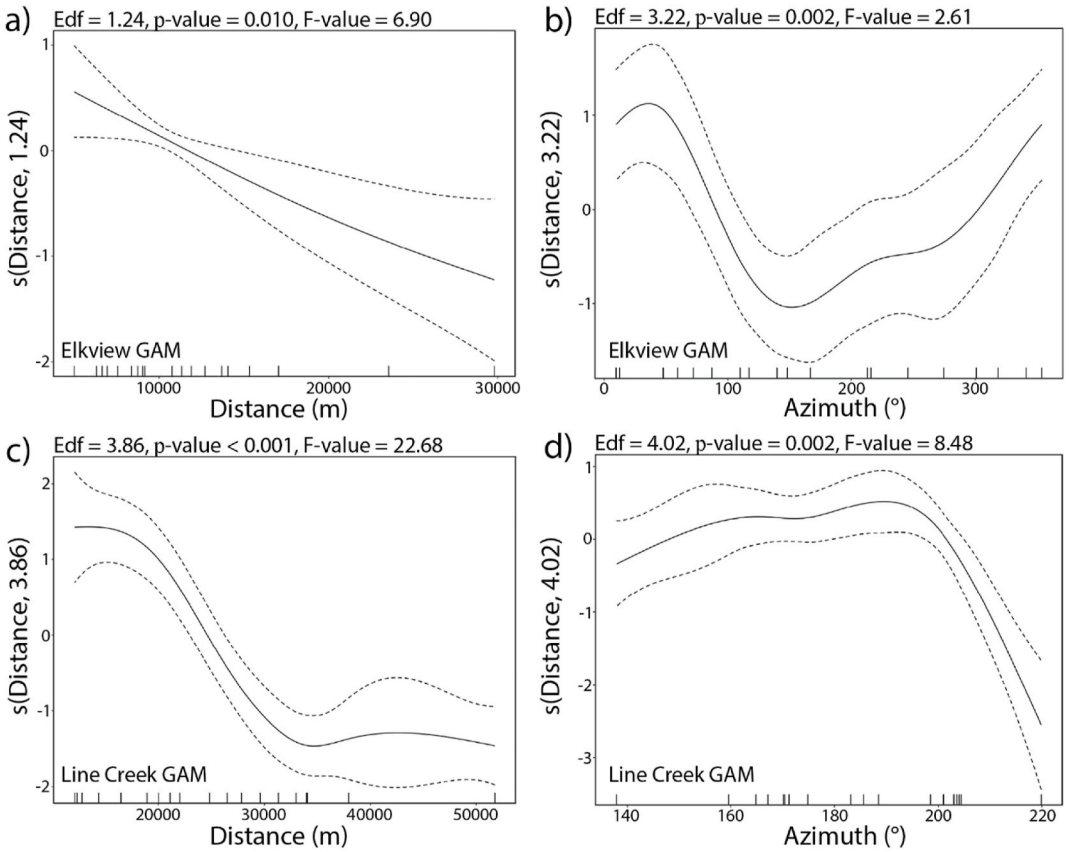

Fig. 2. Generalized additive modelling smooth effect plots for Se contamination throughout the study area as a response to distance and azimuth from either the Elkview Mine (a, b) or Line Creek Mine (c, d). The y-axis represents changes in Se contamination factors, with higher values on the y-axis corresponding to increased Se contamination. Tick marks along the horizontal axis represent sample locations.

near the Line Creek Mine (<10,000 m) as compared to the Elkview Mine. However, because of the low sampling density adjacent to the Line Creek Mine, analysis could not resolve more complex relationships between Se contamination and mine proximity as has been observed in other studies. For example, Ford and Hasselbach (2001) and Hasselbach et al. (2005) observed an exponential relationship between heavy metal contamination and proximity to the Red Dog Mine haul road [43,44]. For the azimuth covariate within the Line Creek GAM, it was also significant (p-value « 0.01) and non-linear (Edf = 4.02; Fig. 2d). Selenium contamination is highest between 160° and 200°, or south of the mine, with a slight decrease in the peak around 175°. On either side of the main curve, Se contamination decreases at azimuths below 160° and above 200°. It should be noted in contrast to the azimuth covariate for the Elkview GAM, which had samples collected between 0° and 360°, the samples collected in relation to the Line Creek Mine only covered azimuth directions between 140° and 220°, which likely explains the rapid decrease in Se contamination at azimuths greater than 200°. The decrease in Se contamination at azimuths less than 160° may be due to regional topography shielding sample locations from the deposition of fugitive dust.

Although the relative percentage of contamination contributed from each of the mines cannot be directly assessed from the methods used in this study, a comparison of the deviance explained, the significant covariates, and regional wind patterns can help us to understand the sources and transport pathways of fugitive dust emissions in the study area. Deviance explained represents the total variance explained by the predictor covariates used in a model. The larger the deviance explained the better the model fits the data. The higher deviance explained within the Line Creek GAM (93.6%) in comparison to the Elkview GAM (77.5%) suggests that a large portion of contamination within the Alexander Creek AMA originates from fugitive dust emissions from the Line Creek Mine. This was further supported by both azimuth covariates indicating contamination was highest south of the Line Creek Mine. Fugitive dust is then transported by the region's prevailing north-south wind patterns leading to the deposition of contaminants south of the mine. A linear regression of Se CFs for samples directly south of the Line Creek Mine in relation to the distance from the Line Creek Mine ($R^2 = 0.88$, p-value <0.01; Figure SI6) supports the notion that contamination in the Alexander Creek AMA primarily originates from the Line Creek Mine as compared to the Elkview Mine (Figure SI7; supplementary information). The steep-walled, mountain ridge, separating the Elkview Mine from samples in the Alexander Creek AMA may account for why a similar linear regression between the distance from the Elkview Mine and Se CFs at samples in the Alexander Creek AMA were not linked, despite the Elkview Mine being more proximal than the Line Creek Mine ($R^2 = 0.14$, p-value = 0.25; Figure SI7). For samples adjacent to the Elkview Mine, contamination is likely

originating from the Elkview Mine as opposed to the Line Creek Mine. For intermediately located samples, especially around the Grave Lake area, the primary source of contamination is harder to disentangle, and contamination is likely sourced from both mines as well as a coal processing and train loadout area that was not analyzed within this study (Fig. 1). It needs to be stressed, however, that both mines along with additional sources of fugitive dust emissions like the region's other mountaintop coal mines, likely supply contaminants throughout the region. However, based on the high deviance explained for the models used within this study it appears a large proportion of Se contamination can be accounted for from either the Elkview or Line Creek mines. Furthermore, it seems that topographic features, like the region's steep-walled north-south running valleys aid in funnelling contamination downwind of the Line Creek Mine but may also help to shield the deposition of some fugitive dust when acting as a geographic barrier between adjacent valleys. This observation is surprising since Cooke and Drevnick (2022) observed increased Se and PACs directly east of the Elkview Mine at Window Mountain Lake, separated by two mountain ridges [9]. When contrasted by Hasselbach et al. (2005) and this study's findings that local topography influences the deposition of heavy metals, primarily that mountain ridges shield the deposition of heavy metals between adjacent valleys, it's clear that more research is required to better understand the controls on transport and deposition of fugitive dust emissions in mountainous regions [44]. Finally, the results from the GAMs demonstrate that contamination is a function of the proximity to mountaintop coal mines, with contamination increasing as distance decreases.

3.3. Other potentially toxic elements

Twenty-seven elements were significantly ($p < 0.01$) correlated to Se with R^2 values greater than 0.50 based on their Pearson correlation coefficients (Table 2). Of the 27 elements, 6 were highly correlated with R^2 values greater than or equal to 0.90 (Table 2, Fig. 3a–f). The concentrations of Se, Ag, Ge, Ni, U, V, and Zr at the most contaminated sites within this study were at contamination levels considered moderate to slightly contaminated as compared to background concentrations. This level of contamination was comparable to other industrially polluted regions around the world [17]. The major difference, however, between this study and others are the maximum concentrations of contaminants at the most contaminated sites. In comparison to sites in Taizhou, China, Ni concentrations are much lower within this study than in sites contaminated by coal-fired industrial plants and other anthropogenic sources, and Cd and Pb concentrations are much lower within this study than at sites along the Red Dog Mine haul road [17,43,44]. However, Ni and V concentrations are higher within this study compared to contaminated sites surrounding open pit mines and upgrading facilities of northern Alberta's Athabasca Bituminous Sands and Elk Island National Park, downwind of Edmonton's petroleum refineries and the Fort Saskatchewan Ni refinery [23]. These differences likely speak to the importance of identifying the sources of contamination but also the methodology used to quantify it. Within the Canadian Council of Ministers of the Environment (CCME) guidelines, there are no guidelines for Se in plant tissues, including mosses relevant to this study that are protective of the environment and human health. CCME guidelines do, however, exist for soil quality in agricultural and residential parkland areas (1 mg/kg dw) and in commercial and industrial areas (2.9 mg/kg dw) [45]. Since the moss tissue analyzed within this study only contains a snapshot of air quality over the last 2–3 years and since the complete uptake of PTEs from fugitive dust emissions cannot be expected, the results from this study should not be used as an absolute measure of contamination. Se and other PTEs have likely accumulated at higher concentrations within soils, for example, as compared to the timeframe captured during moss biomonitoring. It is important then that future studies determine Se concentrations within soils as well as for other PTEs identified in this study to determine if their concentrations exceed CCME soil quality guidelines and if these concentrations pose risks to community and environmental health.

3.4. Potential implications for community health and future work

A growing body of evidence has demonstrated the link between living near surface mining operations, particularly MTR coal mines, and poor community health outcomes [2]. Research has found increased particulate matter produced during mining activities like blasting, dumping of overburden, wind erosion of exposed surfaces, coal-processing, and heavy equipment traffic produce PTEs that led to poor community health outcomes [3,6,45–48]. The U.S. EPA Framework for Metals Risk Assessment overviews metals of primary interest like As, Be, Cd, Cr, Co, Hg, Mn, Ni, Pb, Sb, Se, and V as it relates to the potential for harm to human health and the environment [49]. The results presented within this study demonstrate the strong relationship between proximity and direction from mountaintop coal mines and increased Se contamination consistent with previous research [6,50,51]. Furthermore, PTEs like Ag, Ge, Ni, U, V, and Zr were found to be highly correlated ($R^2 > 0.90$; p-value « 0.01) to Se within this study (Fig. 3). Concentrations of these elements were considered moderate to slightly contaminated, suggesting future research is required to understand the potential risk

Table 2
Pearson correlation coefficients of Se compared to other elements. Contamination factors are presented in brackets for each of the elements for the most contaminated site sampled. All correlated elements with an $R^2 > 0.50$ had p-values <0.05.

R^2	Correlated PTEs with Contamination Factors
$R^2 \geq 0.90$	Ag (4.25), Ge (3.36), Ni (3.49), U (4.06), V (3.46), Zr (2.21)
$0.90 > R^2 \geq 0.80$	Be (2.89), Co (3.33), Cu (1.66), Hf (2.14), Nb (1.74), Y (2.71)
$0.80 > R^2 \geq 0.70$	Ba (3.29), Bi (1.47), Ce (1.37), Fe (1.60), Ga (1.47), La (1.41), Sb (3.53), Sc (2.43)
$0.70 > R^2 \geq 0.60$	As (2.14), Hg (2.65), Pb (2.14), Tl (4.00)
$0.60 > R^2 \geq 0.50$	Cs (2.63), S (1.83), Th (3.12)
$R^2 < 0.50$	Au, Al, B, Ca, Cd, Cr, K, Li, Mg, Mn, Mo, P, Rb, Sn, Sr, Ta, Ti, W, Zn

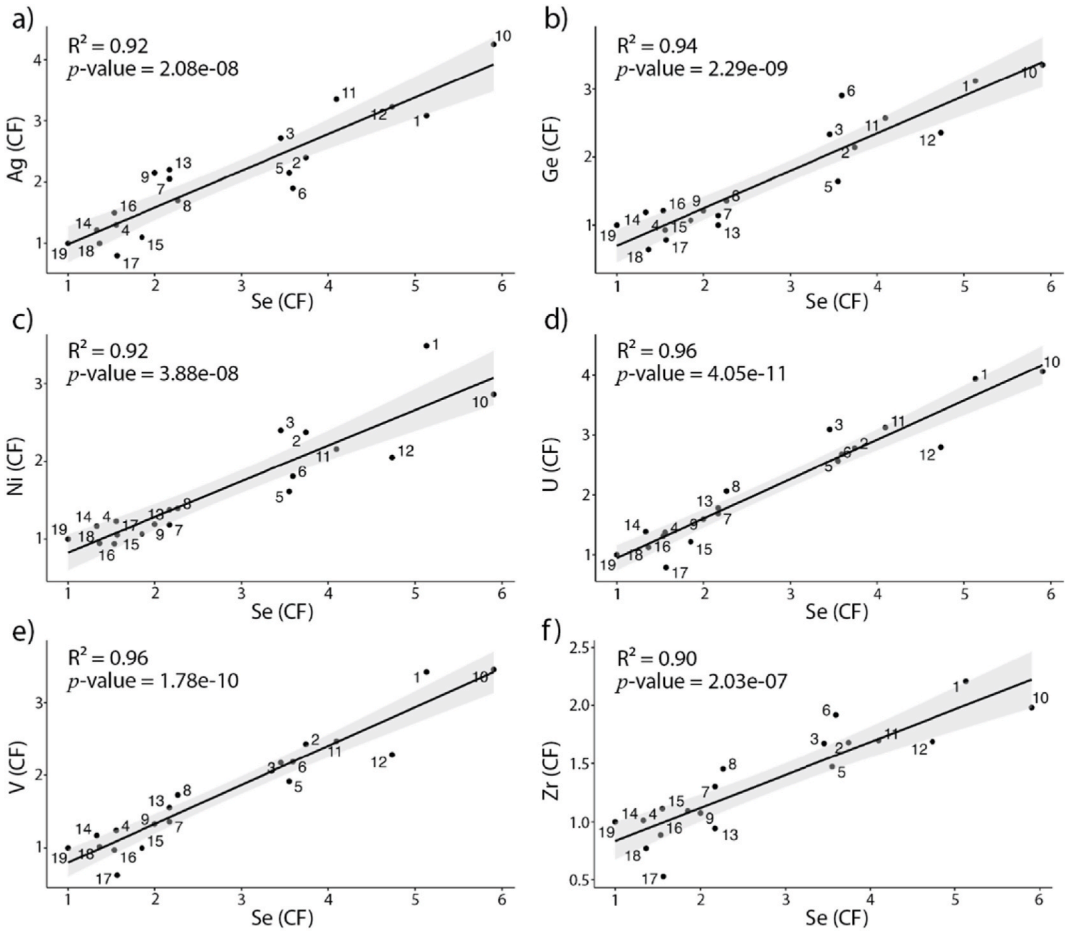

Fig. 3. Scatter plots of Se contamination factors versus Ag (a), Ge (b), Ni (c), U (d), V (e), and Zr (f) contamination factors. Line of best fit is presented with 95% confidence intervals. R^2 and *p*-values correspond to the calculated Pearson correlation coefficients and its significance.

these elements pose to human health and the environment, especially as multiple new mountaintop coal mines are proposed for the region as well as already approved expansions that have the potential to increase fugitive dust emissions in the region. The implications for nearby communities as well as for provincial and federal taxpayers are high as previous research has shown costs associated with poor community health outcomes outweigh the economic benefits of coal mining [52].

There are a number of avenues for future work that could better refine the conclusions of this study. One important avenue will be to determine if the sources of Ni, V, and Se are the same, considering Ni and V are typically indicative of oil combustion emissions [53]. A possible explanation for these associations is that the Se primarily originates from fugitive dust created during physical mining like blasting and dumping of mine waste rock, while Ni and V originate from fugitive dust created during coal-processing and train-loadout operations. Similar findings were found by Ghose and Majee (2007) that attributed different size ranges of total suspended particles to certain mining activities [3]. Examination of PACs throughout the region should also be completed to shed further light on potential sources of fugitive dust emissions and to assess the risk PACs pose to community health as increased exposure to PACs have been documented in other coal mining regions [54]. Finally, analysis that includes the coal geochemistry of the Mist Mountain Formation along with other potential sources of contamination like vehicle-emissions, road dust, and naturally occurring soil constitutes, should be completed to determine the contribution of other sources of contamination to moss and the environment [31].

4. Conclusions

By using moss biomonitoring and generalized additive models this study demonstrated the strong relationship between proximity to mountaintop coal mines and increased Se contamination, including the other potentially toxic elements Ag, Ge, Ni, U, V, and Zr. This study found that contamination was highest immediately surrounding mountaintop mines and decreased at increasing distances from fugitive dust sources. Furthermore, the region's topographic features and prevailing wind patterns likely played a role in the transport and deposition of fugitive dust, but the region's steep mountain ridges may also act in shielding the deposition of some fugitive dust when acting as a geographic barrier between adjacent valleys. Based on the conclusions of this study, other mining jurisdictions in

mountainous regions should be aware of the risk fugitive dust emissions pose to community health and the environment, and the role geographic features may play in controlling the distribution of contaminants.

Author contributions

Wyatt Petryshen: Conceived and designed the experiments; Performed the experiments; Analyzed and interpreted the data; Wrote the paper.

Declaration of competing interest

The authors declare that they have no known competing financial interests or personal relationships that could have appeared to influence the work reported in this paper.

Acknowledgements

The author would like to thank Julian Aherne, Chris Sergeant, and Colin Cooke for valuable discussions and comments on the manuscript. Image used in the graphic abstract is of the Line Creek Mine and was taken by Alec Underwood, Summer 2022. The author would also like to acknowledge contributions from the editorial team and two anonymous peer reviewers for improving the article.

Appendix A. Supplementary data

Supplementary data to this article can be found online at https://doi.org/10.1016/j.heliyon.2023.e17242.

References

[1] M.A. Palmer, E. Bernhardt, W.H. Schlesinger, K.N. Eshleman, E. Foufoula-Georgiou, M.S. Hendryx, A.D. Lemly, G.E. Likens, O.L. Loucks, M.E. Power, P.S. White, P.R. Wilcock, Mountaintop mining consequences, Science 327 (5962) (2010) 148–149.
[2] M. Hendryx, K.J. Zullig, J. Luo, Impacts of coal use on health, Annu. Rev. Publ. Health 41 (2020) 397–415.
[3] M.K. Ghose, S.R. Majee, Characteristics of hazardous airborne dust around an Indian surface coal mining area, Environ. Monit. Assess. 130 (1–3) (2007) 17–25, https://doi.org/10.1007/s10661-006-9448-6.
[4] F. Li, X. Li, L. Hou, A. Shao, Impact of the coal mining on the spatial distribution of potentially toxic metals in farmland tillage soil, Sci. Rep. 8 (2018), 14925, https://doi.org/10.1038/s41598-018-33132-4.
[5] P.B. Tchounwou, C.G. Yedjou, A.K. Patlolla, D.J. Sutton, Heavy metal toxicity and the environment, Experientia Suppl. 101 (2012) 133–164, https://doi.org/10.1007/978-3-7643-8340-4_6.
[6] V.P. Aneja, P.R. Pillai, A. Isherwood, P. Morgan, S.P. Aneja, Particulate matter pollution in the coal-producing regions of the Appalachian Mountains: Integrated ground-based measurements and satellite analysis, J. Air Waste Manag. Assoc. 67 (4) (2017) 421–430, https://doi.org/10.1080/10962247.2016.1245686.
[7] C.C. Wellen, N.J. Shatilla, S.K. Carey, Regional scale selenium loading associated with surface coal mining, Elk Valley, British Columbia, Canada, Sci. Total Environ. 532 (2015) 791–802.
[8] E.K. Sexton, C.J. Sergeant, J.W. Moore, A.R. Westwood, D.M. Chambers, M.V. McPhee, S.A. Nagorski, S.L. O'Neal, J. Weitz, A. Berchtold, M. Capito, C. A. Frissell, J. Hamblen, F.R. Hauer, L.A. Jones, G. Knox, R. Macnair, R.L. Malison, V. Marlatt, J. McIntyre, N. Skuce, D.C. Whited, Canada's mines pose transboundary risks, Science 368 (6489) (2020) 376–377.
[9] C.A. Cooke, P.E. Drevnick, Transboundary atmospheric pollution from mountaintop coal mining, Environ. Sci. Technol. Lett. 9 (11) (2022) 943–948, https://doi.org/10.1021/acs.estlett.2c00677.
[10] Å. Rühling, G. Tyler, An ecological approach to the lead problem, Bot. Not. 121 (1968) 321–342.
[11] Å. Rühling, L. Rasmussen, K. Pilegaard, A. Makinen, E. Steinnes, Survey of atmospheric heavy metal deposition in the Nordic countries in 1985 – monitored by moss analysis, Nord 21 (1987) 1–10.
[12] Å. Rühling, Atmospheric Heavy Metal Deposition in Europe – Estimation Based on Moss Analysis, 1994, Nordic Council of Ministers, Copenhagen, Denmark, 1994.
[13] Å. Rühling, E. Steinnes, Atmospheric Heavy Metal Deposition in Europe 1995 – 1996, 1994, Nordic Council of Ministers, Copenhagen, Denmark, 1998.
[14] H. Harmens, D.A. Norris, E. Steinnes, E. Kubin, R. Piispanen, R. Alber, Y. Aleksiayenak, O. Blum, M. Coşkun, M. Dam, L. De Temmerman, J.A. Fernández, M. Frolova, M. Frontasyeva, L. González-Miqueo, K. Grodzińska, Z. Jeran, S. Korzekwa, M. Krmar, K. Kvietkus, S. Leblond, S. Liiv, S.H. Magnússon, B. Maňkovská, R. Pesch, Å. Rühling, J.M. Santamaria, W. Schröder, Z. Spiric, I. Suchara, L. Thöni, V. Urumov, L. Yurukova, H.G. Zechmeister, Mosses as biomonitors of atmospheric heavy metal deposition: spatial patterns and temporal trends in Europe, Environ. Pollut. 158 (2010) 3144–3156, https://doi.org/10.1016/j.envpol.2010.06.039.
[15] S. Nickel, A. Hertel, R. Persch, W. Schroder, E. Steinnes, H. Uggerud, Modelling and mapping spatio-temporal trends of heavy metal accumulation in moss and natural surface soil monitored 1990-2010 throughout Norway by multivariate generalized linear models and geostatistics, Atmos. Environ. 99 (2014) 85–93.
[16] D.K. Saxena, S. Singh, K. Srivastava, Atmospheric heavy metal deposition in Garhwal Hill area (India): estimation based on native moss analysis, Aerosol Air Qual. Res. (2008) 94–111.
[17] X. Zhou, Q. Chen, C. Liu, Y. Fang, Using moss to assess airborne heavy metal pollution in Taizhou, China, Int. J. Environ. Res. Publ. Health 14 (2017) 430, https://doi.org/10.3390/ijerph14040430.
[18] A.A. Olajira, A survey of heavy metal deposition in Nigeria using moss monitoring methods, Environ. Int. 24 (1998) 951–958.
[19] J.S. Schilling, M.E. Lehman, Bioindication of atmospheric heavy metal deposition in the Southeastern US using the moss Thuidium delicatulum, Atmos. Environ. 36 (10) (2002) 1611–1618, https://doi.org/10.1016/S1352-2310(02)00092-4.
[20] P. Cowden, J. Aherne, Assessment of Atmospheric Metal Deposition by Moss Biomonitoring in a Region under Influence of a Long Standing Active Aluminium Smelter, Atmospheric Environment, 2018, p. 201, https://doi.org/10.1016/j.atmosenv.2018.12.022.
[21] P. Cowden, T. Liang, J. Aherne, Mosses as bioindicators of air pollution along urban-agriculture transect in the Credit River watershed, Southern Ontario, Canada, Ann. Bot. (Rome) 5 (2015) 63–70, https://doi.org/10.4462/annabotrm-13059.
[22] U. Pott, D.H. Turpin, Assessment of atmospheric heavy metals by moss biomonitoring with Isothecium stoloniferum in the Fraser Valley, B.C. Canada. Water, Air, and Soil Pollution 101 (1–4) (1998) 25–44, https://doi.org/10.1023/A:1004916110857.

[23] W. Shotyk, B. Bicalho, C.W. Cuss, M.J.M. Duke, T. Noernberg, R. Pelletier, C. Zaccone, Dust is the dominant source of "heavy metals" to peat moss (Sphagnim fuscum) in the bogs of Athabasca Bituminous Sands region of northern Alberta, Environ. Int. 92–93 (July) (2016) 494–506, https://doi.org/10.1016/j.envint.2016.03.018.

[24] I.C.P. Vegetation, Monitoring of Atmospheric Deposition of Heavy Metals, Nitrogen and POPs in Europe Using Bryophytes, 2015. https://icpvegetation.ceh.ac.uk/publications/documents/MossmonitoringMANUAL-2015-17.07.14.pdf.

[25] Elk Valley Cumulative Effects Management Framework (CEMF) Working Group, Elk Valley Cumulative Effects Assessment and Management Report, 2018. https://www2.gov.bc.ca/gov/content/environment/natural-resource-stewardship/cumulative-effects-framework/regional-assessments/kootenay-boundary/elk-valley-cemf.

[26] G.G. Smith, Coal resources of Canada, Pap. Geol. Surv. Can. 146 (1989).

[27] G. Clarke, B. Northcote, F. Katay, S.P. Tombe, Exploration and mining in British Columbia, 2020: a summary, 2020, in: Provincial Overview of Exploration and Mining in British Columbia, British Columbia Ministry of Energy, Mines and Low Carbon Innovation, British Columbia Geological Survey Information Circular, 2021, pp. 1–45, 2021-01, https://cmscontent.nrs.gov.bc.ca/geoscience/PublicationCatalogue/InformationCircular/BCGS_IC2021-01.pdf.

[28] J.M. Hendry, A. Biswas, J. Essilfie-Dughan, N. Chen, S.J. Day, L.S. Barbour, Reservoirs of selenium in coal waste rock: Elk Valley, British Columbia, Canada, Environ. Sci. Technol. 49 (13) (2015) 8228–8236, https://doi.org/10.1021/acs.est.5b01246.

[29] Teck Resources Ltd, Elk Valley Water Quality Plan 2022 Implementation Plan Adjustment, 2022. https://www.teck.com/media/EVWQP_2022_ImplementationPlanAdjustment_Main_Report.pdf.

[30] J. Essilfie-Dughan, J.M. Hendry, J.J. Dynes, Y. Hu, A. Biswas, L.S. Barbour, S. Day, Geochemical and mineralogical characterization of sulfur and iron in coal waste rock, Elk Valley, British Columbia, Canada, Sci. Total Environ. 586 (2017) 753–769, https://doi.org/10.1016/j.scitotenv.2017.02.053.

[31] F. Goodarzi, D.A. Grieve, H. Sanei, T. Gentzis, N.N. Goodarzi, Geochemistry of coals from the Elk Valley coalfield, British Columbia, Canada, Int. J. Coal Geol. 77 (2002) (2009) 246–259, https://doi.org/10.1016/j.coal.2008.08.010.

[32] Statistics Canada, (table). Census Profile. 2021. Census of Population. Statistics Canada Catalogue no. 98-316-X2021001. Ottawa (2022). Released December 15, 2022, https://www12.statcan.gc.ca/census-recensement/2021/dp-pd/prof/index.cfm?Lang=E.

[33] P. Baillargeon, W.H. Auld, Sparwood Ambient Air Quality Coefficient of Haze Study, Kootenay Regional Operations Waste Management Branch, 1986.

[34] J.R. Aboal, A. Carballeira, A. Casanova, S. Deben, J.A. Fernandez, Quantification of overall measurement uncertainty associated with passive moss biomonitoring technique: sample collection and processing, Environ. Pollut. 224 (2017) 235–242, https://doi.org/10.1016/j.envpol.2017.01.084.

[35] P. Świsłowski, G. Kosior, M. Rajfur, The influence of preparation methodology on the concentrations of heavy metals in Pleurozium schreberi moss samples prior to use in active biomonitoring studies, Environ. Sci. Pollut. Res. Int. 28 (8) (2021) 10068–10076, https://doi.org/10.1007/s11356-020-11484-7.

[36] R Studio Team, RStudio, Integrated Development for R. RStudio, PBC, Boston, MA, 2020. https://www.rstudio.com/.

[37] R Core Team, R: A Language and Environment for Statistical Computing, R Foundation for Statistical Computing, Vienna, Austria, 2021. https://www.R-project.org/.

[38] QGIS.org, QGIS Geographic Information System, QGIS Association, 2022. https://www.qgis.org.

[39] J. Fernández, A. Carballeira, Evaluation of contamination, by different elements, in terrestrial mosses, Arch. Environ. Contam. Toxicol. 40 (2001) 461–468, https://doi.org/10.1007/s002440010198.

[40] C.H. Walker, S.P. Hopkin, R.M. Sibly, D.M. Peakal, Principles of Ecotoxicology, Taylor & Francis, London, 1996.

[41] E.P.R. Gonçalves, R.A.R. Boaventura, C. Mouvet, Sediments and aquatic mosses as pollution indicators of heavy metals in the Ave River basin (Portugal), Sci. Total Environ. 114 (1992) 7–24.

[42] S.N. Wood, Generalized Additive Models: an Introduction with R, 2 edition, Chapman and Hall/CRC, 2017.

[43] J. Ford, L. Hasselbach, Heavy Metals in Mosses and Soils on Six Transacts along the Red Dog Mine Haul Road Alaska, May 2001, Western Arctic National Parklands National Park Service, Alaska, 2001, https://www.google.com/url?sa=t&rct=j&q=&esrc=s&source=web&cd=&ved=2ahUKEwi6u7mW_p3_AhXwBTQIHWBJAzEQFnoECAoQAQ&url=https%3A%2F%2Fdec.alaska.gov%2Fmedia%2F15042%2Freddogrpt2.pdf&usg=AOvVaw0b_C6xFTuYXid4bQqjHoVi.

[44] L. Hasselbach, J.M. Ver Hoef, J. Ford, P. Neitlich, E. Crecelius, S. Berryman, B. Wolk, T. Bohle, Spatial patterns of cadmium and lead deposition on and adjacent to National Park Service lands in the vicinity of Red Dog Mine, Alaska, Sci. Total Environ. 348 (2005) 211–230, https://doi.org/10.1016/j.scitotenv.2004.12.084.

[45] CCME, Canadian Soil Quality Guidelines: Selenium. Environmental and Human Health. Scientific Supporting Document, Canadian Council of Ministers of the Environment, Winnipeg, 2009.

[46] S. Luanpitpong, M. Chen, T. Knuckles, S. Wen, J. Luo, E. Ellis, M. Hendryx, Y. Rojanasakul, Appalachian mountaintop mining particulate matter induces neoplastic transformation of human bronchial epithelial cells and promotes tumor formation, Environ. Sci. Technol. 48 (21) (2014) 12912–12919, https://doi.org/10.1021/es504263u.

[47] V.P. Aneja, A. Isherwood, P. Morgan, Characterization of particulate matter (PM10) related to surface coal mining operations in Appalachia, Atmos. Environ. 54 (2012) 96–501, https://doi.org/10.1016/j.atmosenv.2012.02.063.

[48] R.B. Finkelman, Modes of occurrence of environmentally-sensitive trace elements in coal, in: D.J. Swaine, F. Goodarzi (Eds.), Environmental Aspects of Trace Elements in Coal, Energy & Environment, vol. 2, Springer, Dordrecht, 1995, https://doi.org/10.1007/978-94-015-8496-8_3.

[49] U.S. Environmental Protection Agency, Framework for Metals Risk Assessment, 2007. EPA 120/R-07/001, https://www.epa.gov/sites/default/files/2013-09/documents/metals-risk-assessment-final.pdf.

[50] M. Hendryx, The public health impacts of surface coal mining, Extr. Ind. Soc. 2 (2015) 820–826, https://doi.org/10.1016/j.exis.2015.08.006.

[51] L.M. Kurth, M. McCawley, M. Hendryx, S. Lusk, Atmospheric particulate matter size distribution and concentration in West Virginia coal mining and non-mining area, J. Expo. Sci. Environ. Epidemiol. 24 (2014) 405–411, https://doi.org/10.1038/jes.2014.2.

[52] M. Hendryx, M.M. Ahern, Mortality in appalachian coal mining regions: the value of statistical life lost, Public Health Reports, July - August 2009 124 (2009) 541–550.

[53] N.F. Surprenant, W. Battye, D. Roeck, S.M. Sandberg, Emissions Assessment of Conventional Stationary Combustion Systems: Volume V: Industrial Combustion Sources, U.S. Environmental Protection Agency. Washington D.C., 1981. EPA/600/7-81/003c (NTIS PB81225559).

[54] M. Hendryx, S. Wang, K.A. Romanak, A. Salamova, M. Venier, Personal exposure to polycyclic aromatic hydrocarbons in Appalachian mining communities, Environmental pollution (Barking, Essex: 1987) 257 (2020), 113501, https://doi.org/10.1016/j.envpol.2019.113501.